

CALCULATION OF THERMAL AND ELECTRIC FIELDS
IN LARGE-DIAMETER INGOTS UNDER VARIABLE
CONDITIONS OF ELECTRICAL SLAG MELTING

G. F. Ivanova

UDC 536.421.1:621.365.3

The procedure shown in [1] for calculating thermal fields is applied to ingots with large diameters. Numerical results are obtained for two such ingots.

In [1] we have formulated the thermal and electrical problem of the electrical slag melting process, have proposed a procedure for numerical calculations, and have shown an illustrative calculation of the temperature field in a small-diameter laboratory ingot. A somewhat modified procedure is used for calculating large-diameter industrial ingots under variable melting conditions, including the formation of shrinkage cavities. Without delving into the mathematical description of the problem, we will now bring out only those modifications which pertain to large-diameter ingots.

In the original formulation of the problem in [1] it was assumed that droplets of metal trickling from the electrode onto the ingot surface release heat (if $T \leq \Theta_2$) or absorb heat (if $T > \Theta_2$) at the ingot surface. For calculating large-diameter ingots we assume that droplets of metal at temperature Θ_2 fall into a metal bath and penetrate deeper into it, with all their heat becoming distributed uniformly within the region

$$D = \{0 \leq r \leq R_1, H < z < H + H_d, T \geq \Theta_0\},$$

where the depth of droplet penetration H_d is assumed equal to half the depth of the liquid metal pool. In view of this, in the equation of heat conduction for an ingot at points of region D there appears a term $g_1(T)$ which represents the volume concentration of heat sources:

$$g_1(T) = \frac{R_2^2 v(t) c_0 \rho_0 (\Theta_2 - T)}{R_1^2 H_d}.$$

In calculating industrial ingots it is necessary to consider the possibility of variable melting conditions, when the voltage u^* applied to the electrode varies as some function of time. Since stabilization of the electric field in a slag bath occurs usually much faster than the variation of voltage $u^*(t)$ at the electrode, hence in the steady-state electrical problem one may replace the unknown voltage $u(r, z, t)$ by a new unknown function $\varphi(r, z) = u(r, z, t)/u^*(t)$. Function $\varphi(r, z)$ is described by the steady-state Laplace equation with boundary conditions which are independent of time t . For the concentration of heat sources in a slag bath we obtain the following expression:

$$g(r, z, t) = \frac{1}{\rho} u^{*2}(t) \left\{ \left(\frac{\partial \varphi}{\partial r} \right)^2 + \left(\frac{\partial \varphi}{\partial z} \right)^2 \right\}. \quad (1)$$

In this way, having once solved the problem for φ and having thus also determined the field of its derivatives with respect to r and z , we find the field of heat sources at every instant of time t from formula (1).

For a numerical solution of the thermal problem one uses the Peaceman-Rackford method of variable directions [2], taking into account the latent heat of phase transformation [3, 4] by the Oleinik-Kamenomostskaya method. For solving the problem of determining function φ , the Laplace equation is replaced by the equation $\Delta \varphi = \partial \varphi / \partial t$ and the steady-state solution is found by the same Peaceman-Rackford method.

Computer Center at the P. Stuchki Latvian State University, Riga. Translated from *Inzhenerno-Fizicheskii Zhurnal*, Vol. 22, No. 2, pp. 706-710, April, 1972. Original article submitted May 19, 1971.

© 1974 Consultants Bureau, a division of Plenum Publishing Corporation, 227 West 17th Street, New York, N. Y. 10011. No part of this publication may be reproduced, stored in a retrieval system, or transmitted, in any form or by any means, electronic, mechanical, photocopying, microfilming, recording or otherwise, without written permission of the publisher. A copy of this article is available from the publisher for \$15.00.

TABLE 1. Variables v_i , T_{\max} , H_3 , H_4 , and z_i as Functions of Time for Ingots with Diameters 1100 mm and 1500 mm

t, h	$v_i(t)$, m/h	T_{\max} , °C	H_3 , m	H_4 , m	$z_i(t)$, m
Ingot diameter 1100 mm					
1,8	0,265	2611	0,048	0,276	0,41
3,6	0,259	2584	0,045	0,569	0,89
5,4	0,256	2549	0,037	0,747	1,35
6,3	0,247	2523	0,035	0,778	1,58
7,2	0,245	2508	0,027	0,791	1,80
10,8	0,161	2311	0,005	0,621	2,55
12,6	0,132	2211	0,013	0,480	2,81
Ingot diameter 1500 mm					
1,8	0,287	2372	0,13	0,252	0,41
4,5	0,227	2236	0,12	0,695	1,10
7,2	0,185	2146	0,10	0,910	1,65
8,1	0,166	2120	0,063	0,930	1,81
12,6	0,135	2046	0,016	0,772	2,47
15,3	0,121	2011	0,013	0,668	2,82
18,0	0,109	1984	0,010	0,580	3,13

2. We will show the results of numerical calculations made for two steel ingots with diameters 1100 mm and 1500 mm, respectively. The initial values for the 1100 mm ingot are: $R_1 = R_2 = 0.4375$ m, $R = 0.55$ m, $h = 0.05$ m, $H = 0.46$ m, $l = 0.01$ m, $\eta = 0.008$ m, $\rho_1 = 2500$ kg/m³, $\rho_0S = 7600$ kg/m³, $\rho_0L = 6900$ kg/m³, $c_1S = c_0L = 838$ J/kg·°C, $c_1L = 1466.5$ J/kg·°C, $c_0S = 586.6$ J/kg·°C, $k_1S = 2.33$ J/m·sec·°C, $k_1L = 168.8$ J/m·sec·°C, $k_0S = 39.6$ J/m·sec·°C, $k_0L = 79.2$ J/m·sec·°C, $\Theta_0 = 1500^\circ\text{C}$, $\Theta_1 = \Theta_2 = 1650^\circ\text{C}$, $\varepsilon_0 = 0.8$, $\varepsilon_1 = 0.7$, $\gamma = 2.4 \cdot 10^5$ J/kg, $u_0 = u_2 = 20^\circ\text{C}$, $u_1 = 1600^\circ\text{C}$, $T_0 = T_1 = 100^\circ\text{C}$, $T_2 = T_3 = 150^\circ\text{C}$, $T_4 = T_5 = 20^\circ\text{C}$, $\alpha_2 = \alpha_3 = 408$ J/m²·sec·°C, $\rho_S = 2.8$ Ω·m, $\rho_L = 0.00324$ Ω·m;

$$u^*(t) = \begin{cases} 65, & 0 \leq t \leq 8, \\ -2t + 85, & 8 \leq t \leq 12, \\ 55, & t > 12 \end{cases}$$

($u^*(t)$ in volts). The initial values for the 1500 mm ingot differ from those for the 1100 mm ingot inasmuch as here $R_1 = R_2 = 0.6$ m, $R = 0.75$ m, $h = 0.19$ m, $H = 0.56$ m, and $\alpha_2 = \alpha_3 = 128$ J/m²·sec·°C;

$$u^*(x) = \begin{cases} -11.5x + 70, & x \leq 1.26, \\ -7.08x + 64.425, & 1.26 \leq x \leq 2.46, \\ -3.75x + 56.225, & x \geq 2.46, \end{cases}$$

$$x = H + l + z_i(t).$$

The ingot begins to melt after 41 min in the 1100 mm ingot and after 54 min in the 1500 mm ingot.

The linear casting rate of an ingot v_i , the core temperature of a slag bath T_{\max} , the height of the cylindrical portion of a liquid metal bath H_3 , the depth of the liquid metal pool in the bath H_4 , and the height of the cast ingot z_i are all shown in Table 1, as functions of time, for the 1100 mm and the 1500 mm ingot.

The test data for the 1100 mm ingot include the trend of the $T = 1465^\circ\text{C}$ isotherm (solidus line) and the height of the cast ingot after $t = 3.6$ h and $t = 6.3$ h. The calculated and measured data are compared in Fig. 1. The discrepancy between the calculated and the measured depth of the liquid metal pool after 3.6 and 6.3 h is 8 and 12%, respectively, while the discrepancy in the height of a cast ingot after the same melting times is 6 and 8%, respectively.

Of great practical importance in the casting of ingots is the final stage of the process: the proper choice of the operating voltage mode $u^*(t)$ during the final, to avoid the formation of shrinkage cavities which would form if the metal on the ingot surface were solid while inside the metal there still existed a liquid region. For the 1100 mm ingot we show the results of the following melting mode: I) $u^*(t) = 0$ at $t \geq 12.6$ h and II) $u^*(t) = -9.167t + 170.5$ at $12.6 \leq t \leq 18.6$ h. The changes in the $T = 1500^\circ\text{C}$ isotherm for the ingot ($z \geq 0.46$) under conditions I) and II) are shown in Fig. 2. In mode I), when the voltage during the final stage is switched off instantly, already 1 h later ($t = 13.7$ h) there forms a large shrinkage cavity. If the voltage during the final stage is decreased linearly from 55 V down to zero within 6 h (mode II)), however, then no shrinkage cavity forms and the ingot is completely crystallized within 2.8 h of the final stage. In Fig. 2 is also shown the shift of the $T = 1340^\circ\text{C}$ melting isotherm for slag in the slag bath ($0 \leq z < 0.46$) under mode II).

Calculations for the 1500 mm ingot were made according to the following operating modes: III) $u^*(t) = -8.4775t + 195$ at $18 \leq t \leq 23$ h and IV) $u^*(t) = -5.3t + 137.76$ at $18 \leq t \leq 26$ h. A shrinkage cavity is produced after 3 h of the final stage ($t = 21$ h) in mode III) and after 4 h in mode IV). The size of the shrinkage cavity is much smaller in mode IV) than in mode III).

It is to be noted that calculations for the final stage are based on the same electric potential field (normalized to unity) as calculations for the entire process, although at the end, when the slag bath begins to cool and a solid slag crust appears, the potential field undergoes changes. In calculating the concentrations of heat sources $g(r, z, t)$, however, the resistivity is assumed ρ_S for the solid phase and ρ_L for

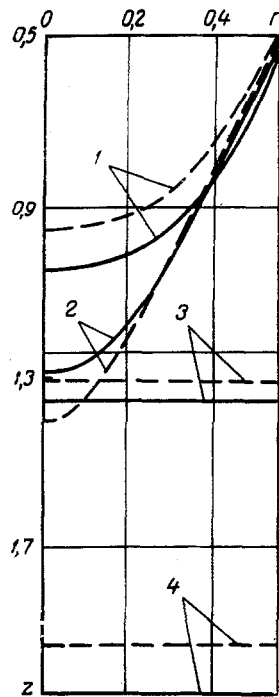


Fig. 1

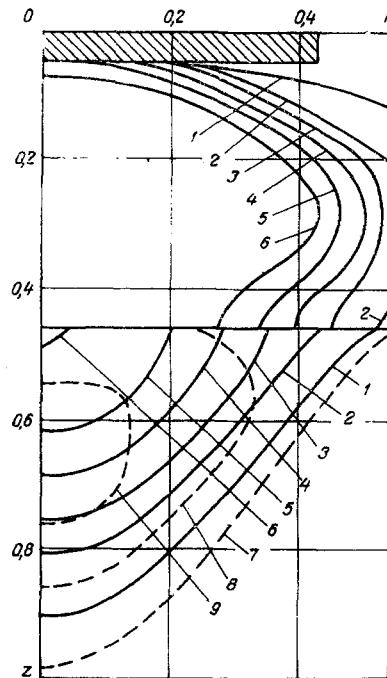


Fig. 2

Fig. 1. Comparison between test values (dashed line) and calculated values (solid line) for the 1100 mm ingot (r, z , in m): 1, 2) trends of the 1465°C isotherm; 3, 4) heights of the cast ingot; 1, 3) $t = 3.6$ h; 2, 4) $t = 6.3$ h.

Fig. 2. Shift of the $T = 1340^\circ\text{C}$ melting isotherm for slag and of the $T = 1500^\circ\text{C}$ melting isotherm for metal, as a function of time, for the 1100 mm ingot during formation of shrinkage cavities [in mode II), solid line, and in mode I), dotted line]: 1) $t = 13$ h; 2) 13.7 h; 3) 14 h; 4) 14.3 h; 5) 14.7 h; 6) 15 h; 7) 12.6 h; 8) 13 h; 9) 13.7 h; $r, m; z, m$.

the liquid phase. Inasmuch as ρ_S and ρ_L differ by almost three orders of magnitude, heat sources are in effect eliminated from the solid slag and this seems to agree closely with actual conditions.

Thus, the procedure developed here yields the temperature field in laboratory as well as in industrial ingots under various melting conditions. The calculations were made on a BESM-4 computer.

NOTATION

R_1, R_2, R	are the radii of the pool, the electrode, and the ingot, respectively;
h	is the depth of the electrode penetration into the slag;
H	is the height of the slag bath;
H_3	is the height of the cylindrical portion of the liquid metal bath;
H_d	is the depth of the droplet penetration;
η	is the thickness of the slag crust;
l	is the thickness of the mold;
ρ_1, ρ_0S, ρ_0L	are the densities of the slag, the solid metal, and the liquid metal, respectively;
$c_{1S}, c_{1L}, c_{0S}, c_{0L}$	are the specific heats of the slag and the metal, respectively;
$k_{1S}, k_{1L}, k_{0S}, k_{0L}$	are the thermal conductivities;
ϵ_0, ϵ_1	are the emissivities of the metal and slag, respectively;
γ	is the latent heat of the fusion;
Θ_0	is the melting temperature of the metal;
Θ_1	is the superheat temperature of the metal;
Θ_2	is the temperature of the metal droplet after passage through the slag bath;
u_0, u_1, u_2	are the initial temperatures of the electrode, the slag, and the metal, respectively;

T_{\max}	is the core temperature of the slag bath;
T_0, T_1, \dots, T_5	are the ambient temperatures at the respective segments of the ingot wall;
α_2, α_3	are the coefficients of the heat transfer at the wall Γ_2 and Γ_3 , respectively;
ρ_L, ρ_S	are the electrical resistivities of the liquid and the solid slag, respectively;
u^*	is the electrode potential (voltage);
v_i	is the linear casting rate;
z_i	is the height of the cast ingot.

LITERATURE CITED

1. G. F. Ivanova and N. A. Avdonin, *Inzh.-Fiz. Zh.*, 20, No. 1 (1971).
2. N. N. Yanenko, *Method of Fractional Steps in Solving Multidimensional Problems of Mathematical Physics* [in Russian], Nauka (1967), pp. 26-29.
3. O. A. Oleinik, *Dokl. Akad. Nauk SSSR*, 135, No. 5 (1960).
4. S. L. Kamenomostskaya, *Matem. Sb.*, 53, No. 4 (1961).